

REFERENCES AND NOTES

- B. K. Burgess, D. J. Lowe, *Chem. Rev.* **96**, 2983–3012 (1996).
- J. B. Howard, D. C. Rees, *Proc. Natl. Acad. Sci. U.S.A.* **103**, 17088–17093 (2006).
- L. C. Seefeldt, B. M. Hoffman, D. R. Dean, *Annu. Rev. Biochem.* **78**, 701–722 (2009).
- M. M. Georgiadis *et al.*, *Science* **257**, 1653–1659 (1992).
- J. Kim, D. C. Rees, *Nature* **360**, 553–560 (1992).
- H. Schindelin, C. Kisker, J. L. Schlessman, J. B. Howard, D. C. Rees, *Nature* **387**, 370–376 (1997).
- J. W. Peters, K. Fisher, W. E. Newton, D. R. Dean, *J. Biol. Chem.* **270**, 27007–27013 (1995).
- D. J. Lowe, K. Fisher, R. N. F. Thorneley, *Biochem. J.* **292**, 93–98 (1993).
- O. Einsle *et al.*, *Science* **297**, 1696–1700 (2002).
- T. Spatzal *et al.*, *Science* **334**, 940 (2011).
- K. M. Lancaster *et al.*, *Science* **334**, 974–977 (2011).
- Y. Hu, M. W. Ribbe, *Coord. Chem. Rev.* **255**, 1218–1224 (2011).
- D. C. Rees *et al.*, *Philos. Trans. A Math. Phys. Eng. Sci.* **363**, 971–984 (2005).
- D. J. Lowe, R. N. F. Thorneley, *Biochem. J.* **224**, 895–901 (1984).
- R. N. F. Thorneley, D. J. Lowe, *Biochem. J.* **215**, 393–403 (1983).
- J. Chatt, J. R. Dilworth, R. L. Richards, *Chem. Rev.* **78**, 589–625 (1978).
- J. C. Hwang, C. H. Chen, R. H. Burris, *Biochim. Biophys. Acta* **292**, 256–270 (1973).
- L. M. Cameron, B. J. Hales, *Biochemistry* **37**, 9449–9456 (1998).
- L. C. Davis, M. T. Henzl, R. H. Burris, W. H. Orme-Johnson, *Biochemistry* **18**, 4860–4869 (1979).
- C. C. Lee, Y. Hu, M. W. Ribbe, *Science* **329**, 642–642 (2010).
- Y. Hu, C. C. Lee, M. W. Ribbe, *Science* **333**, 753–755 (2011).
- H.-I. Lee, L. M. Cameron, B. J. Hales, B. J. Hoffman, *J. Am. Chem. Soc.* **119**, 10121–10126 (1997).
- L. Yan *et al.*, *Eur. J. Inorg. Chem.* **2011**, 2064–2074 (2011).
- S. J. George, G. A. Ashby, C. W. Wharton, R. N. F. Thorneley, *J. Am. Chem. Soc.* **119**, 6450–6451 (1997).
- Z. Maskos, B. J. Hales, *J. Inorg. Biochem.* **93**, 11–17 (2003).
- R. C. Pollock *et al.*, *J. Am. Chem. Soc.* **117**, 8686–8687 (1995).
- L. C. Davis, M. T. Henzl, R. H. Burris, W. H. Orme-Johnson, *Biochemistry* **18**, 4860–4869 (1979).
- D. W. Mulder *et al.*, *Structure* **19**, 1038–1052 (2011).
- P. M. C. Benton *et al.*, *Biochemistry* **42**, 9102–9109 (2003).
- C. H. Kim, W. E. Newton, D. R. Dean, *Biochemistry* **34**, 2798–2808 (1995).
- P. C. Dos Santos, S. M. Mayer, B. M. Barney, L. C. Seefeldt, D. R. Dean, *J. Inorg. Biochem.* **101**, 1642–1648 (2007).
- D. J. Scott, H. D. May, W. E. Newton, K. E. Brigle, D. R. Dean, *Nature* **343**, 188–190 (1990).
- J. Christiansen, V. L. Cash, L. C. Seefeldt, D. R. Dean, *J. Biol. Chem.* **275**, 11459–11464 (2000).
- J. Rittle, J. C. Peters, *Proc. Natl. Acad. Sci. U.S.A.* **110**, 15898–15903 (2013).
- I. Dance, *Chem. Asian J.* **2**, 936–946 (2007).

ACKNOWLEDGMENTS

We thank J. Peters, L. Zhang, J. Rittle, C. Morrison, B. Wenke, and K. Dörner for informative discussions. This work was supported by NIH grant GM45162 (D.C.R.), Deutsche Forschungsgemeinschaft grants EI-520/7 and RTG 1976, and the European Research Council N-ABLE project (O.E.). We gratefully acknowledge the Gordon and Betty Moore Foundation, the Beckman Institute, and the Sanofi-Aventis Bioengineering Research Program at Caltech for their generous support of the Molecular Observatory at Caltech and the staff at Beamline 12-2, Stanford Synchrotron Radiation Lightsource (SSRL), for their assistance with data collection. SSRL is operated for the U.S. Department of Energy and supported by its Office of Biological and Environmental Research and by the NIH: National Institute of General Medical Sciences (P41GM103393) and the National Center for Research Resources (P41RR001209). We thank the Center for Environmental Microbial Interactions for its support of microbiology research at Caltech. Coordinates and structure factors have been deposited in the Protein Data Bank of the Research Collaboratory for Structural Bioinformatics, with IDs 4TKV (Av1-CO) and 4TKU (Av1 reactivated).

SUPPLEMENTARY MATERIALS

www.sciencemag.org/content/345/6204/1620/suppl/DC1
Materials and Methods
Figs. S1 and S2
Tables S1 and S2
References (36–43)

29 May 2014; accepted 31 July 2014
10.1126/science.1256679

IMMUNODEFICIENCY

Immune dysregulation in human subjects with heterozygous germline mutations in *CTLA4*

Hye Sun Kuehn,^{1*} Weiming Ouyang,^{2*} Bernice Lo,^{3,4*} Elissa K. Deenick,^{5,6} Julie E. Niemela,¹ Danielle T. Avery,⁵ Jean-Nicolas Schickel,⁷ Dat Q. Tran,⁸ Jennifer Stoddard,¹ Yu Zhang,^{4,9} David M. Frucht,² Bogdan Dumitriu,¹⁰ Phillip Scheinberg,¹⁰ Les R. Folio,¹¹ Cathleen A. Frein,¹² Susan Price,^{3,4} Christopher Koh,¹³ Theo Heller,¹³ Christine M. Seroogy,¹⁴ Anna Huttenlocher,^{14,15} V. Koneti Rao,^{3,4} Helen C. Su,^{4,9} David Kleiner,¹⁶ Luigi D. Notarangelo,¹⁷ Yajesh Rampertaap,¹⁸ Kenneth N. Olivier,¹⁸ Joshua McElwee,¹⁹ Jason Hughes,¹⁹ Stefania Pittaluga,¹⁶ Joao B. Oliveira,²⁰ Eric Meffre,⁷ Thomas A. Fleisher,^{1†} Steven M. Holland,^{4,18} Michael J. Lenardo,^{3,4†} Stuart G. Tangye,^{5,6} Gulbu Uzel^{18†}

Cytotoxic T lymphocyte antigen-4 (CTLA-4) is an inhibitory receptor found on immune cells. The consequences of mutations in *CTLA4* in humans are unknown. We identified germline heterozygous mutations in *CTLA4* in subjects with severe immune dysregulation from four unrelated families. Whereas *Ctla4* heterozygous mice have no obvious phenotype, human *CTLA4* haploinsufficiency caused dysregulation of FoxP3⁺ regulatory T (T_{reg}) cells, hyperactivation of effector T cells, and lymphocytic infiltration of target organs. Patients also exhibited progressive loss of circulating B cells, associated with an increase of predominantly autoreactive CD21^{lo} B cells and accumulation of B cells in nonlymphoid organs. Inherited human *CTLA4* haploinsufficiency demonstrates a critical quantitative role for CTLA-4 in governing T and B lymphocyte homeostasis.

Immune tolerance is controlled by multiple mechanisms (1, 2), including regulatory T (T_{reg}) cells (3–5) and inhibitory receptors (6, 7). T_{reg} cells constitutively express the inhibitory receptor CTLA-4, which confers suppressive functions (8, 9). CTLA-4, also known as CD152, is also expressed by activated T cells and, upon ligation, inhibits their proliferation (10). Homozygous deficiency of *Ctla4* in mice causes fatal multiorgan lymphocytic infiltration and destruction (11–13); hence, CTLA-4 functions at a key “checkpoint” in immune tolerance. CTLA-4–immunoglobulin (Ig) fusion protein and neutralizing CTLA-4 antibody are used to modulate immunity in autoimmune and cancer patients (14, 15), respectively. Studies have given conflicting results regarding the association of *CTLA4* single-nucleotide variants (SNVs) with organ-specific autoimmunity (16). The consequences of genetic CTLA-4 deficiency in humans are unknown.

Our index patient—a 22-year-old female (A.I.I.1)—developed brain, gastrointestinal (GI), and lung lymphocytic infiltrates, autoimmune thrombocytopenia, and hypogammaglobulinemia in early childhood (Fig. 1A and table S1). Her 43-year-old father (A.I.I.1) manifested lung and GI infiltrates, hypogammaglobulinemia, and clonally expanded $\gamma\delta$ -CD8⁺ T cells infiltrating and suppressing the bone marrow (fig. S1A). Four additional cases from three unrelated families (families B, C, and D) (fig. S1 and table S1) were identified among a cohort of 23 patients with autoimmune cytopenias, hypogammaglobulinemia, CD4 T cell lymphopenia, and lymphocytic infiltration of non-lymphoid organs. Patient B.I.1, previously diagnosed with common variable immunodeficiency

¹Department of Laboratory Medicine, Clinical Center, National Institutes of Health, Bethesda, MD 20892, USA. ²Laboratory of Cell Biology, Division of Monoclonal Antibodies, Office of Biotechnology Products, Center for Drug Evaluation and Research, U.S. Food and Drug Administration, Bethesda, MD 20892, USA. ³Molecular Development of the Immune System Section, Laboratory of Immunology, National Institute of Allergy and Infectious Diseases, Bethesda, MD 20892, USA. ⁴NIAD Clinical Genomics Program, National Institute of Allergy and Infectious Diseases, Bethesda, MD 20892, USA. ⁵Immunology and Immunodeficiency Group, Immunology Division, Garvan Institute of Medical Research, Sydney, NSW 2010, Australia. ⁶St. Vincent's Clinical School Faculty of Medicine, University of New South Wales, Sydney, NSW 2010, Australia. ⁷Department of Immunobiology, Yale University School of Medicine, New Haven, CT 06511, USA. ⁸Department of Pediatrics, University of Texas Medical School, Houston, TX 77030, USA. ⁹Immunological Diseases Unit, Laboratory of Host Defenses, National Institute of Allergy and Infectious Diseases, Bethesda, MD 20892, USA. ¹⁰Hematology Branch, National Heart, Lung and Blood Institute, Bethesda, MD 20892, USA. ¹¹Radiology and Imaging Sciences, Clinical Center, National Institutes of Health, Bethesda, MD 20892, USA. ¹²Clinical Research Directorate, Clinical Monitoring Research Program, Leidos Biomedical Research Inc., Frederick National Laboratory for Cancer Research, Frederick, MD 21702, USA. ¹³Liver Diseases Branch, National Institute of Diabetes and Digestive and Kidney Diseases, Bethesda, MD 20892, USA. ¹⁴Department of Pediatrics, University of Wisconsin, Madison, WI 53706, USA. ¹⁵Department of Medical Microbiology and Immunology, University of Wisconsin, Madison, WI 53706, USA. ¹⁶Laboratory of Pathology, National Cancer Institute, Bethesda, MD 20892, USA. ¹⁷Division of Immunology and Manton Center for Orphan Disease Research, Children's Hospital, Harvard Medical School, Boston, MA 02127, USA. ¹⁸Laboratory of Clinical Infectious Diseases, National Institute of Allergy and Infectious Diseases, Bethesda, MD 20892, USA. ¹⁹Merck Research Laboratories, Merck & Co., Boston, MA 02130, USA. ²⁰Instituto de Medicina Integral Prof. Fernando Figueira—IMIP, 50070 Recife-PE, Brazil.

*These authors contributed equally to this work.

†Corresponding author. E-mail: tfleishe@cc.nih.gov (T.A.F.); lenardo@nih.gov (M.J.L.); guzel@niaid.nih.gov (G.U.)

Fig. 1. Clinical phenotype and pedigree of the patients. (A) Top: Computed tomography images of lung and brain from patient A.II.1. Bottom: Histological section (magnification 20×) from a duodenal biopsy from a healthy donor (HD) and patient A.II.1 stained for CD3 (brown cells), showing an increased number of transepithelial T cells within the villi. (B) Flow cytometric analyses of CD4⁺ cells or total lymphocytes stained for the indicated surface markers from a healthy donor (HD) and patient A.II.1. Data showing decreased CD45RA⁺CD62L⁺ naive CD4⁺ T cells are representative of three patients (A.I.1, A.II.1, and B.I.1). Programmed cell death-1 (PD1) expression data shown are representative of five patients (A.I.1, A.II.1, B.I.1, C.II.1, and D.II.1) and three healthy donors. Data showing decreased circulating B cells are representative of two patients (A.I.1 and A.II.1). (C) Mutations in patient alleles displayed on a schematic of the four exons of *CTLA4*, pedigrees, and phenotype summary highlighting organs (gray) with inflammatory infiltrates and autoimmune cytopenias for affected family members. TM, transmembrane domain. (D) Protein and mRNA expression of CTLA-4 in T_{reg} cells. Left: Levels of CTLA-4 expression in T_{reg} cells (CD4⁺CD25⁺FoxP3⁺) were assessed by intracellular staining. The numbers in the upper right corner depict mean fluorescence intensity (MFI) of anti-CD152 (CTLA-4) staining. Dotted line indicates the peak of CTLA-4 expression in a healthy donor. Data shown are representative of three experiments. Right: Levels of *CTLA4* mRNA in T_{reg} cells (CD4⁺CD25⁺CD127^{lo}) sorted from seven different healthy donors and four patients were measured by real-time PCR using the probe for *CTLA4* transcript variant 1 (full length) and normalized to GAPDH. Data are means of replicates from six experiments. For relative gene expression, all data were normalized to the same HD. The horizontal lines indicate mean values from healthy donors or patients.

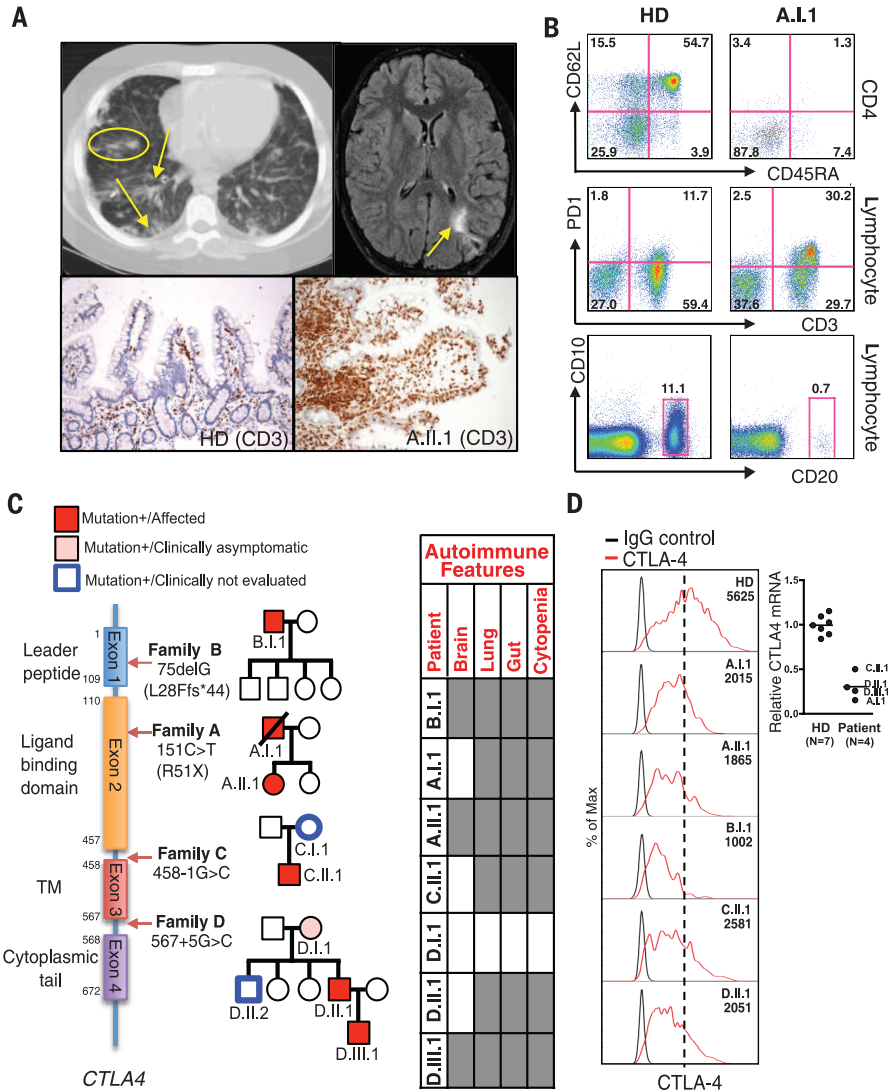
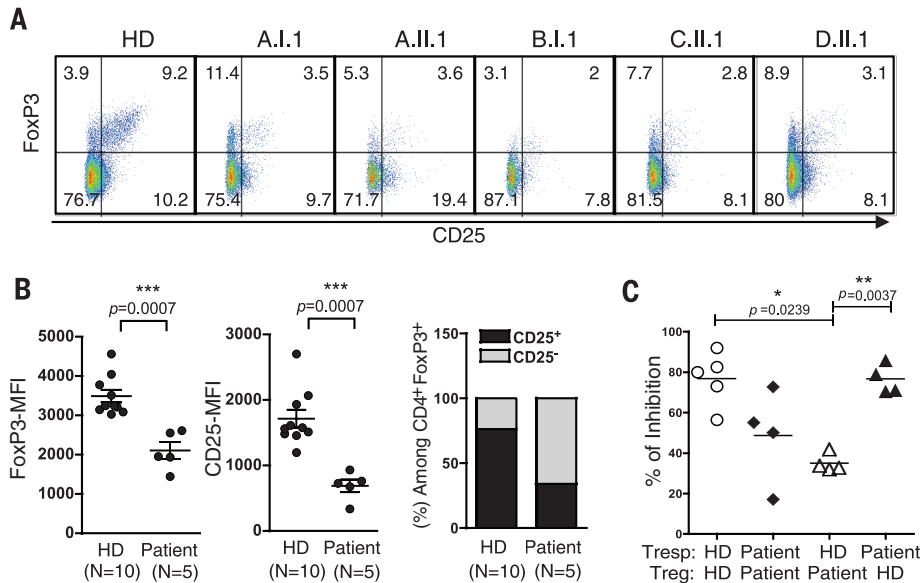


Fig. 2. Abnormal T_{reg} cell phenotype and function in patients. (A) Flow cytometric analysis of FoxP3 and CD25 in CD4⁺ T cells from healthy donor (HD) and patients. (B) Mean fluorescence intensity of FoxP3 and CD25 in CD4⁺ FoxP3⁺ T cells from healthy donors and patients. Data are means ± SEM of replicates of indicated patient [A.I.1 (N = 7), A.II.1 (N = 1), B.I.1 (N = 2), C.II.1 (N = 2), D.II.1 (N = 4)] and 10 healthy donors. The N values represent number of replicates from each patient. ***P = 0.0007 (Mann-Whitney test). Bar graph: Percentage of CD25⁺ and CD25⁻ cells among CD4⁺FoxP3⁺ in 10 healthy donors and five patients. (C) Autologous and heterologous suppressive activities of T_{reg} cells from five healthy donors and four patients (A.I.1, B.I.1, C.II.1, and D.II.1). The horizontal lines indicate the mean values. Data are from three experiments, with each indicated patient paired with one or two healthy donors. *P = 0.0239, **P = 0.0037 (paired t test).



(CVID), had hepatosplenomegaly, autoimmune hemolytic anemia (AIHA), autoimmune thrombocytopenia, pulmonary nodules, and cerebral infiltrative lesions. C.II.1, a 19-year-old male, had childhood-onset EBV⁺ Hodgkin's lymphoma and developed diffuse lymphadenopathy, splenomegaly, AIHA, autoimmune thrombocytopenia, and enteropathy. His mother (C.I.1), asymptomatic and considered unaffected, consented to genomic studies only. Patient D.II.1 is a 46-year-old male with psoriasis, lymphadenopathy, AIHA, and manifested GI and lung lymphocytic infiltrates. His mother (D.I.1) was unaffected, and his brother (D.II.2) was reportedly healthy but not clinically evaluated; however, his 11-year-old son (D.III.1) had lymphadenopathy, severe AIHA, and lymphocytic brain infiltration. In most patients, GI biopsies revealed histopathology similar to that caused by CTLA-4 blocking antibody treatment in melanoma patients (17, 18).

Both patients in family A had low CD4⁺ T cells with depleted CD45RA⁺CD62L⁺ naïve cells, increased expression of the exhaustion marker PD-1,

and a progressive loss of circulating mature B cells (Fig. 1B and table S1). Similar and overlapping immune phenotypes were detected in the additional families (Fig. 1, B to D, and table S1).

We performed whole-exome sequencing using DNA from A.II.1 and identified a heterozygous, nonsense c.151C>T (p.R51X) mutation in *CTLA4*. This was confirmed by Sanger sequencing in the proband and A.I.1 (Fig. 1C). cDNA analyses from A.I.1 T cells showed that the mutant allele mRNA was degraded >95%, consistent with nonsense-mediated decay (table S2). *CTLA4* sequencing in B.I.1 revealed a frameshift deletion (c.75delG; p.L28Ffs*44) (Fig. 1C) that introduced a stop codon in exon 2. Families C and D had mutations in introns 2 and 3 (458-1G>C and 567+5G>C) (Fig. 1C) disrupting the acceptor and donor sites of the second or third introns, respectively. These mutations generated a *CTLA4* mRNA lacking the third exon, putatively encoding a soluble form of *CTLA4* (fig. S2A). Full-length *CTLA4* mRNA, encoding the membrane-bound form, was reduced. Serum-soluble CTLA-4 was comparable in patients

and healthy individuals. In an extended cohort, de novo mutants were not identified; however, because B.I.1's parental genotypes are unknown, his mutation could be de novo.

Affected patients had reduced CTLA-4 protein and mRNA expression in sorted T_{reg} cells relative to healthy donors; this reduction persisted after activation (Fig. 1D and fig. S2, A and B). Deletion of *Ctla4* in mice impairs T_{reg} cell suppressive function, causing severe autoimmune disease and early lethality despite normal Foxp3 levels (11, 12). We found that patients had normal percentages of Foxp3⁺ T_{reg} cells with a CD127⁺CD45RO⁺Helios⁺ phenotype (fig. S3, A and B), but overall expressed significantly less Foxp3 and CD25 [interleukin-2 (IL-2) receptor α subunit and a marker of T_{reg} cells] than T_{reg} cells from healthy donors, and a large proportion of their T_{regs} were CD25⁻ (Fig. 2, A and B). *FOXP3* mRNA was also reduced in patient T_{reg} cells (fig. S3C). Next, we tested the function of healthy donor or patient T_{reg} cells and found that patient T_{regs} poorly suppressed proliferation of cocultured

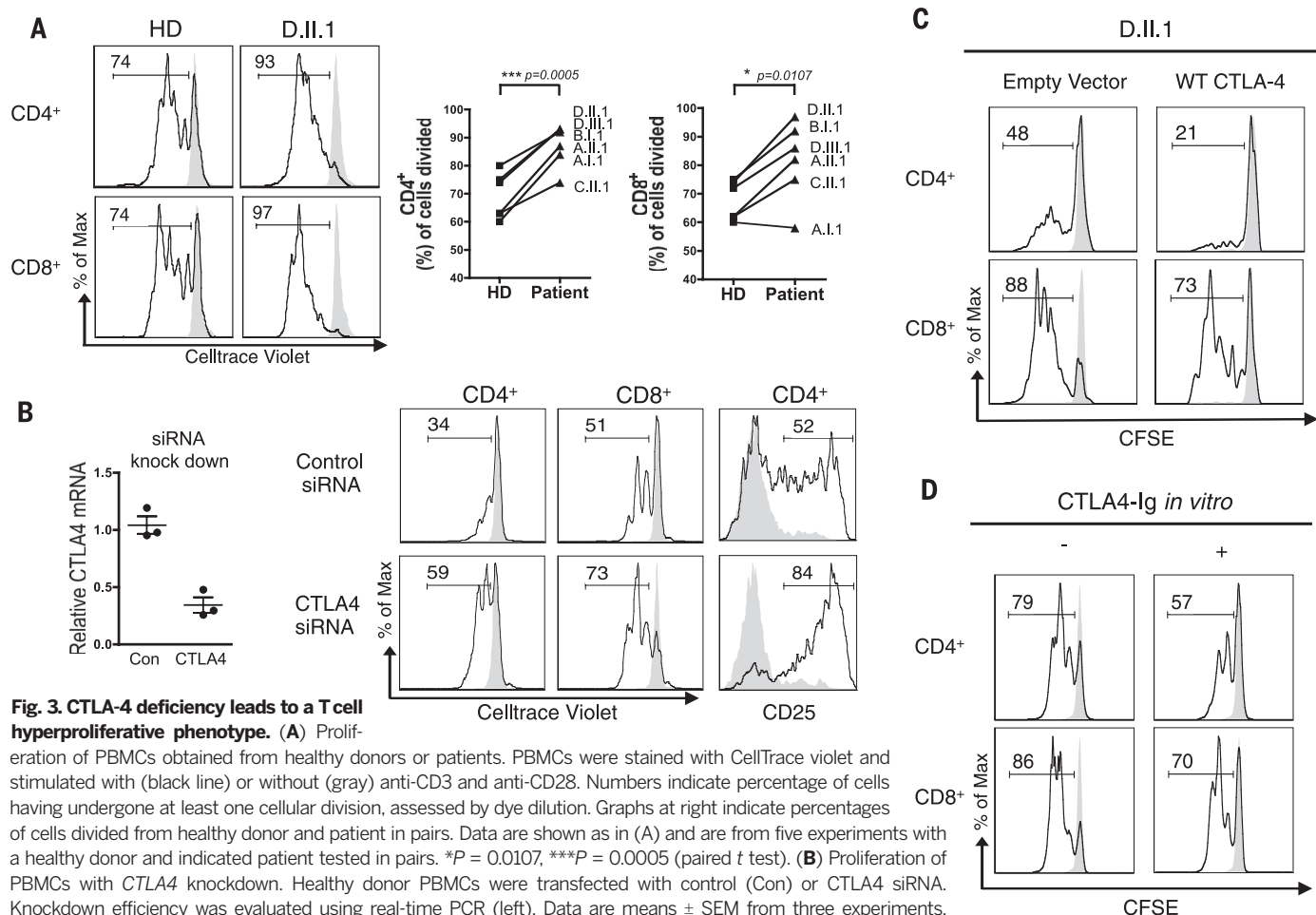


Fig. 3. CTLA-4 deficiency leads to a T cell hyperproliferative phenotype. (A) Proliferation of PBMCs obtained from healthy donors or patients. PBMCs were stained with CellTrace violet and stimulated with (black line) or without (gray) anti-CD3 and anti-CD28. Numbers indicate percentage of cells having undergone at least one cellular division, assessed by dye dilution. Graphs at right indicate percentages of cells divided from healthy donor and patient in pairs. Data are shown as in (A) and are from five experiments with a healthy donor and indicated patient tested in pairs. * $P = 0.0107$, *** $P = 0.0005$ (paired t test). (B) Proliferation of PBMCs with *CTLA4* knockdown. Healthy donor PBMCs were transfected with control (Con) or CTLA4 siRNA. Knockdown efficiency was evaluated using real-time PCR (left). Data are means \pm SEM from three experiments, each with a different healthy donor. Cells were then assessed for proliferation and CD25 expression. Data shown are representative of three experiments with three healthy donors tested. (C) Reconstitution of wild-type CTLA-4 in patient cells. Patient D.II.1 PBMCs were transfected with control vector (pDsRed-N1) or CTLA-4-DsRed-N1 vector. Proliferation of DsRed⁺ CD4 and CD8 patient T cells. Data shown are representative of three experiments with a total of three patients (B.I.1, C.II.1, D.II.1). (D) Effect of in vitro treatment with CTLA-4-Ig on proliferation of PBMCs. Patient D.II.1 PBMCs were stimulated with anti-CD3 in the presence (+) or absence (-) of CTLA-4-Ig. Data shown are representative of three experiments with a total of three patients (B.I.1, D.II.1, and D.III.1). Percentages of cells having undergone at least one cellular division are indicated in each histogram. Gray peak shows unstimulated cells.

activated autologous or allogeneic T responder cells (Fig. 2C and fig. S3D).

Among the nine subjects harboring *CTLA4* mutations, three relatives were reportedly healthy (C.I.1, D.I.1, and D.II.2). Only one of these unaffected healthy relatives (D.I.1) could be evaluated in detail, and she had no clinical findings similar to CTLA-4-deficient patients. Her T_{reg} cells showed higher expression of CTLA-4 and normal levels of FoxP3 and CD25 (fig. S4, A and B), whereas her effector T cells displayed the same *in vitro* hyperproliferation observed in affected patients (fig. S4C); these findings suggest that T_{reg} cell dysfunction might be essential for the full disease phenotype.

Consistent with the results of studies in mice (11–13), CTLA-4-deficient patient T cells were hyperproliferative, with an increased percentage expressing CD25 in response to T cell receptor stimulation (Fig. 3A and fig. S5A). To test whether patient T cell hyperproliferation resulted from reduced *CTLA4* expression, we used small interfering RNA (siRNA) to inhibit *CTLA4* expression in normal peripheral blood mononuclear cells (PBMCs). A factor of ~3 reduction in *CTLA4* recapitulated the hyperproliferative T cell phenotype (Fig. 3B). Moreover, overexpression of wild-type CTLA-4 in patient T cells suppressed the hyperproliferation (Fig. 3C and fig. S5, B and C), indicating that quantitative variations in CTLA-4 controlled the proliferative potential of T cells. CTLA-4-Ig fusion protein also suppressed patient T cell proliferation *in vitro* (Fig. 3D). Despite hyperproliferation of patient T cells in culture, the patients were lymphopenic. This may be explained by increased FAS (CD95) expression, caspase activity, and apoptosis of patient T cells, or by organ sequestration (fig. S6).

CTLA-4 function in B cells has been investigated, but its role remains unclear (8, 12, 19). We found that CTLA-4 expression was significantly reduced on activated B cells from patients (fig. S7A). The reduced frequencies of CD27⁺ class-switched memory B cells and progressive B cell lymphopenia (Fig. 4, A and B), together with known B cell abnormalities in human autoimmune diseases (20), prompted us to further investigate B cell maturation and function.

In inflammatory conditions such as systemic lupus erythematosus, rheumatoid arthritis, Sjögren's syndrome, CVID with autoimmunity and lymphoproliferation, and certain chronic infections, a population of B cells expressing reduced levels of CD21 (termed CD21^{lo} B cells) has been identified (21–23). CD21^{lo} B cells have been viewed as anergic or “exhausted” cells on the basis of observations such as enrichment of self-reactive B cell receptors (BCRs), an activated phenotype, reduced responsiveness to BCR engagement, and increased apoptosis (22–25). We found that the frequency of CD21^{lo} B cells was greatly elevated in patients' peripheral blood (Fig. 4B) (15 to 90% of B cells in CTLA-4-deficient patients versus <5% in controls). This subset progressively accumulated in patient A.I.1 from 41.5% to >95% of peripheral blood B cells over 3 years. Consistent with the anergic/exhausted state of CD21^{lo} B cells (22), we observed heightened apoptosis in patient B cells (fig. S7, B and C) and poor BCR-induced proliferation relative to controls (Fig. 4C). The CD21^{lo} B cells in CTLA-4-deficient patients were CD19^{hi}CD20^{hi}CD38^{lo}, distinguishing them from transitional (CD19⁺CD20^{hi}CD38^{hi}) cells. Flow cytometric analysis revealed that these cells were phenotypically similar to the CD21^{lo} B cell subset in other immune dysregulation disorders (fig.

S8A) (21, 25). Accordingly, autoreactive IgG may be produced by the CD21^{lo} B cells, as a greater proportion were IgG⁺CD27⁺ cells, relative to the corresponding cells in healthy donors. Functional analysis *in vitro* indicated that naïve B cells from CTLA-4-deficient patients secreted IgM and underwent class switching to secrete IgG and IgA robustly (fig. S8B). However, patient CD21^{lo} B cells secreted less Ig than those of healthy donors (fig. S8B). The propensity of CD21^{lo} B cells to exhibit more apoptosis *ex vivo* (fig. S7C) and their constitutive expression of CD95 (fig. S8A) could explain peripheral B cell lymphopenia and hypogammaglobulinemia in most CTLA-4-deficient patients. Increased frequencies of autoreactive mature naïve B cells have been demonstrated in the blood of patients with immunodysregulation polyendocrinopathy enteropathy X-linked syndrome (IPEX), which is a primary T_{reg} cell defect (26); this suggests a role for T_{reg} cells in preventing the accumulation of autoreactive B cells in the periphery. Thus, CTLA-4 haploinsufficiency decreases B cell tolerance and survival either intrinsically or extrinsically because of T_{reg} dysfunction (26).

Our data indicate that germline *CTLA4* haploinsufficiency causes lymphoproliferation, lymphocytic infiltration of nonlymphoid organs, autoimmune cytopenias, and B cell abnormalities with an accumulation of CD21^{lo} B cells. These cells may account for antibody-mediated autoimmunity in our patients. In contrast, heterozygous *Ctla4* deficiency in mice shows no obvious phenotype (12, 13). Interestingly, patient D.I.1, who has a *CTLA4* splicing mutation with no apparent somatic reversions or leakiness, is clinically healthy (table S2). This incomplete penetrance in disease may result from other genetic differences

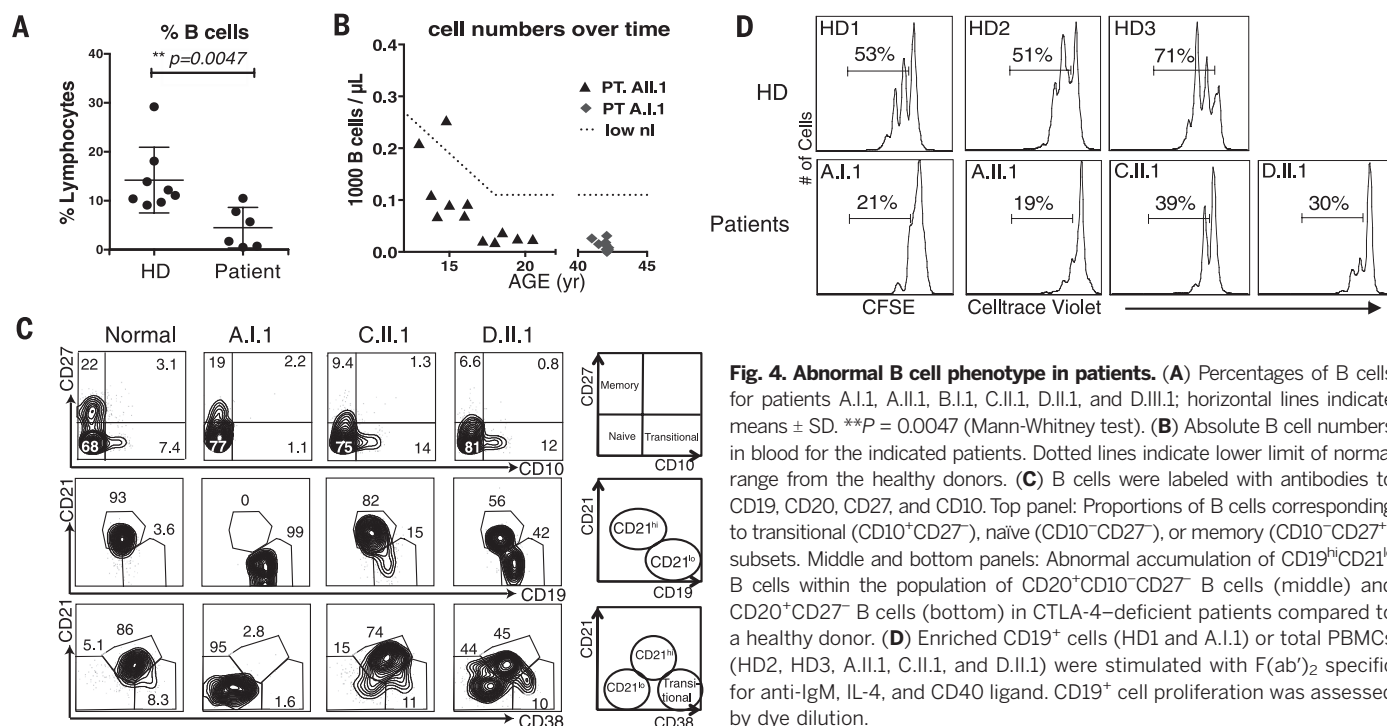


Fig. 4. Abnormal B cell phenotype in patients. (A) Percentages of B cells for patients A.I.1, A.II.1, B.I.1, C.II.1, D.II.1, and D.III.1; horizontal lines indicate means \pm SD. ***P* = 0.0047 (Mann-Whitney test). (B) Absolute B cell numbers in blood for the indicated patients. Dotted lines indicate lower limit of normal range from the healthy donors. (C) B cells were labeled with antibodies to CD19, CD20, CD27, and CD10. Top panel: Proportions of B cells corresponding to transitional (CD10⁺CD27⁺), naïve (CD10⁺CD27⁺), or memory (CD10⁺CD27⁺) subsets. Middle and bottom panels: Abnormal accumulation of CD19^{hi}CD21^{lo} B cells within the population of CD20⁺CD10⁺CD27⁺ B cells (middle) and CD20⁺CD27⁺ B cells (bottom) in CTLA-4-deficient patients compared to a healthy donor. (D) Enriched CD19⁺ cells (HD1 and A.I.1) or total PBMCs (HD2, HD3, A.II.1, C.II.1, and D.II.1) were stimulated with F(ab')₂ specific for anti-IgM, IL-4, and CD40 ligand. CD19⁺ cell proliferation was assessed by dye dilution.

between family members. This is analogous to that in autoimmune lymphoproliferative syndrome, a human genetic immune disorder with only 60% penetrance among family members harboring the same heterozygous gene mutation (27). Contrary to genetic deficiencies in inbred strains of mice, phenotypic variability is commonly observed in human single-gene disorders (28). This may explain why D.I.1 has a *CTLA4* mutation, yet is asymptomatic. C.I.1 and D.II.2 are apparently healthy because of incomplete penetrance; however, further immunological testing is required to confirm this assumption. We did not identify any common genetic modifiers in this study, as proven by our cohort analysis (see supplementary text). Also, our analysis of nonsynonymous SNVs in the *CTLA4* coding region showed that CTLA-4 expression and T cell function are comparable to those of wild-type controls (table S3 and figs. S9 and S10). Nonetheless, our findings show that the mutations reported here result in quantitative reductions in CTLA-4 expression, which contribute to a severe loss of tolerance and infiltrative autoimmune disease.

Our results show the spectrum of clinical complications that can be anticipated from CTLA-4–blocking drugs. Consistent with these findings, treatment with the CTLA-4 mimetic, CTLA-4-Ig, suppressed patient T cell hyperproliferation in vitro (Fig. 3D) and could be a potential therapeutic intervention for CTLA-4–deficient patients. Taken together, our results show that heterozygous *CTLA4* mutations in humans

are associated with a severe immunoregulatory disorder, which we term CTLA-4 haploinsufficiency with autoimmune infiltration (CHAI) disease.

REFERENCES AND NOTES

1. J. A. Bluestone *et al.*, *Nat. Rev. Immunol.* **10**, 797–803 (2010).
2. C. C. Goodnow, *Cell* **130**, 25–35 (2007).
3. S. Sakaguchi, T. Yamaguchi, T. Nomura, M. Ono, *Cell* **133**, 775–787 (2008).
4. S. Z. Josefowicz, L. F. Lu, A. Y. Rudensky, *Annu. Rev. Immunol.* **30**, 531–564 (2012).
5. C. Benoist, D. Mathis, *Cold Spring Harb. Perspect. Biol.* **4**, a007021 (2012).
6. B. T. Fife, J. A. Bluestone, *Immunol. Rev.* **224**, 166–182 (2008).
7. L. Chen, D. B. Flies, *Nat. Rev. Immunol.* **13**, 227–242 (2013).
8. K. Wing *et al.*, *Science* **322**, 271–275 (2008).
9. O. S. Qureshi *et al.*, *Science* **332**, 600–603 (2011).
10. M. F. Krummel, J. P. Allison, *J. Exp. Med.* **183**, 2533–2540 (1996).
11. E. A. Tivol *et al.*, *Immunity* **3**, 541–547 (1995).
12. P. Waterhouse *et al.*, *Science* **270**, 985–988 (1995).
13. C. A. Chambers, T. J. Sullivan, J. P. Allison, *Immunity* **7**, 885–895 (1997).
14. G. Herrero-Beaumont, M. J. Martínez Calatrava, S. Castañeda, *Rheumatol. Clin.* **8**, 78–83 (2012).
15. M. K. Callahan, J. D. Wolchok, J. P. Allison, *Semin. Oncol.* **37**, 473–484 (2010).
16. H. Ueda *et al.*, *Nature* **423**, 506–511 (2003).
17. P. Attia *et al.*, *J. Clin. Oncol.* **23**, 6043–6053 (2005).
18. G. Q. Phan *et al.*, *Proc. Natl. Acad. Sci. U.S.A.* **100**, 8372–8377 (2003).
19. D. Quandt, H. Hoff, M. Rudolph, S. Fillatreau, M. C. Brunner-Weinzierl, *J. Immunol.* **179**, 7316–7324 (2007).
20. D. A. Kaminski, C. Wei, Y. Qian, A. F. Rosenberg, I. Sanz, *Front. Immunol.* **3**, 302 (2012).
21. M. Rakhmanov *et al.*, *Proc. Natl. Acad. Sci. U.S.A.* **106**, 13451–13456 (2009).

22. I. Isnardi *et al.*, *Blood* **115**, 5026–5036 (2010).
23. K. Warnatz *et al.*, *Blood* **99**, 1544–1551 (2002).
24. C. C. Goodnow, R. Brink, E. Adams, *Nature* **352**, 532–536 (1991).
25. S. Moir *et al.*, *J. Exp. Med.* **205**, 1797–1805 (2008).
26. T. Kinnunen *et al.*, *Blood* **121**, 1595–1603 (2013).
27. S. Price *et al.*, *Blood* **123**, 1989–1999 (2014).
28. M. E. Conley, J. L. Casanova, *Curr. Opin. Immunol.* **30**, 17–23 (2014).

ACKNOWLEDGMENTS

We thank the referring physicians, as well as the patients and families. The data are tabulated in the main paper and in the supplementary materials. Supported by the Intramural Research Program, NIH Clinical Center (H.S.K., T.A.F., J.S., J.E.N., L.R.F.); the Division of Intramural Research, National Institute of Allergy and Infectious Diseases (B.L., Y.Z., V.K.R., H.C.S., Y.R., K.N.O., S.Pr., S.M.H., M.J.L., G.U.); the National Cancer Institute under contract HHSN261200800001E (C.A.F.); National Institute of Allergy and Infectious Diseases grant 5R01HL113304-01 (D.Q.T.); the National Health and Medical Research Council of Australia (E.K.D., S.G.T.); Cancer Council NSW (S.G.T.); and National Institute of Allergy and Infectious Diseases grants AI071087, AI095848, and AI061093 (E.M.). The content of this publication does not necessarily reflect the views or policies of the U.S. Department of Health and Human Services, nor does mention of trade names, commercial products, or organizations imply endorsement by the U.S. Government. The sequencing data are deposited in dbGaP under accession no. phs000797.v1.p1.

SUPPLEMENTARY MATERIALS

www.sciencemag.org/content/345/6204/1623/suppl/DC1
Materials and Methods
Supplementary Text
Figs. S1 to S10
Tables S1 to S3
References (29–35)

12 May 2014; accepted 2 September 2014
Published online 11 September 2014;
10.1126/science.1255904